Atmos. Chem. Phys. Discuss., https://doi.org/10.5194/acp-2017-1090
Manuscript under review for journal Atmos. Chem. Phys.
Discussion started: 19 December 2017

Atmospheric Chemistry and Physics Discussions

Turbulent Characteristics of Saltation and Uncertainty of Saltation Model Parameters

Dongwei Liu[1], Masahide Ishizuka[2], Yaping Shao[3*]

[1]School of Ecology and Environment, Inner Mongolia University, China
liudw@imu.edu.cn
[2]Faculty of Engineering, Kagawa University, Japan
ishizuka@eng.kagawa-u.ac.jp
[3]Institute for Geophysics and Meteorology, University of Cologne, Germany
yshao@uni-koeln.de

Abstract: It is widely recognized that saltation is a turbulent process, similar to other transport processes in the atmospheric boundary layer. But due to the lack of high frequency observations, the statistic behavior of saltation is so far not well understood. In this study, we use the data from the Japan-Australian Dust Experiment (JADE) to investigate turbulent saltation by analyzing the probability density function, energy spectrum and intermittency of saltation fluxes. Threshold friction velocity, u_{*t}, and saltation coefficient, c_0, are two important parameters in saltation models, often assumed to be deterministic. But as saltation is turbulent, we argue that it is more reasonable to consider them as parameters obeying certain probability distributions. The JADE saltation fluxes are used to estimate the u_{*t} and c_0 probability distributions. The stochasticity of these parameters is attributed to the randomness in friction velocity and threshold friction velocity as well as soil particle size.

Keywords: wind erosion; turbulent saltation; saltation intermittency; saltation model; threshold friction velocity; saltation coefficient; maximum likelihood

Highlight: We use the data from a field experiment to investigate saltation by analysing the probability density function, energy spectrum and intermittency of saltation fluxes. We also estimate two key wind-erosion model parameters and their probabilistic distributions. It continues the line of considering saltation as a turbulent process and represents a progress towards deriving more general wind erosion models.

1. Introduction

It is known from the start of modern aeolian research [Bagnold, 1941] that saltation, the hop motion of sand grains near the earth's surface, is a turbulent process. However, early aeolian studies focused mainly on its "mean" behaviour. Most well-known is for example the Owen [Owen, 1964] saltation model which predicts that the vertically integrated saltation flux is proportional to friction velocity cubed. A dedicated investigation on turbulent saltation was conducted by Butterfield [1991]. Staut and Zobeck [1997] introduced the idea of saltation intermittency and pointed out that even when the averaged friction velocity, u_*, is below the threshold, saltation can still intermittently occur. The emphasis of the latter authors has been on the saltation intermittency caused by the fluctuations of turbulent wind. Turbulent saltation has attracted much attention in more recent years [e.g. McKenna Neuman et al. 2000; Davidson-Arnott and Bauer, 2009; Sherman et al. 2017] and sophisticated models have been under developed to model the process [e.g. Dupond et al. 2013]. However, due to the lack of high-frequency field observations of saltation fluxes, the statistical behaviour of turbulent saltation is to date not well understood.

Atmos. Chem. Phys. Discuss., https://doi.org/10.5194/acp-2017-1090
Manuscript under review for journal Atmos. Chem. Phys.
Discussion started: 19 December 2017

Atmospheric Chemistry and Physics Discussions

A related problem is how saltation can parameterized in wind erosion models. For example, for dust modelling, it is important to quantify saltation, as saltation bombardment is a main mechanism for dust emission. In wind erosion models, threshold friction velocity, u_{*t}, is a key parameter which depends on many factors including soil texture, moisture, salt concentration, crust and surface roughness. In models, it is often expressed as

$$u_{*_t}(d;\lambda,\theta,s_l,c_r,\ldots) = u_{*_t}(d)\, f_\lambda(\lambda)\, f_w(\theta)\, f_{sc}(s_l)\, f_{cr}(c_r)\ldots \quad (1)$$

where $u_{*t}(d)$ is the minimal threshold friction velocity for grain size d [Shao and Lu, 2000]; λ is roughness frontal-area index; θ is soil moisture; s_l is soil salt content and c_r is a descriptor of surface crustiness; f_λ, f_w, f_{sc} and f_{cr} are the corresponding correction functions. The corrections are determined semi-empirically, e.g., f_λ using the Raupach et al. [1993] scheme and f_w the Fécan et al. [1999] scheme. The corrections f_{sc} and f_{cr} are so far not well known.

For homogeneous saltation, the saltation flux can be computed using the Kawamura [1964] scheme, here multiplied by the fraction of erodible surface area σ_f,

$$Q(d) = \begin{cases} \sigma_f c_o \dfrac{\rho}{g}\, u_*^3 \left(1-\dfrac{u_{*_t}}{u_*}\right)\left(1+\dfrac{u_{*_t}}{u_*}\right)^2 & u_* > u_{*_t} \\ 0 & \text{otherwise} \end{cases} \quad (2)$$

where d is particle diameter in sand particle size range, ρ is air density, g is acceleration due to gravity and u_* is friction velocity. According to Kawamura [1964], the saltation coefficient, c_o, falls between 1.8 and 3.1. In wind-erosion models, c_o is often set to 2.6 [White, 1979]. The total (all particle size) saltation flux, Q, is a particle-size weighted average of $Q(d)$

$$Q = \int_{d_1}^{d_2} Q(d)\, p_s(d)\, \delta d \quad (3)$$

where d_1 and d_2 define the upper and lower limits of saltation particle size, respectively, and $p_s(d)$ is the soil particle size distribution. Observations show, however, c_o varies considerably from case to case, and as the data presented later in this paper show, for a given location, it may vary from day to day and even during a wind erosion event.

While wind-erosion modules built in numerical weather and global climate models [e.g. Shao et al. 2011; Kok et al. 2014; Klose et al. 2014] are in general more sophisticated than what is described above and include a dust scheme, the estimate of Q is essentially done using Equations (1) to (3) or similar. Thus, the estimates of u_{*t} and specification of c_0 are rather critical to wind-erosion and dust modelling.

In most wind erosion models, both u_{*t} and c_o are considered to be deterministic. But as saltation is turbulent, it is more rational to treat u_{*t} and c_o as parameters which satisfy certain probability distributions. Saltation intermittency also implies that u_{*t} and c_0 must depend on the scale of averaging. Shao and Mikami [2005] noticed that u_{*t} for 10-minute averaged Q and 1-minute averaged Q are quite different. Namikas et al. [2003] and Ellis et al. [2012] have also noticed that averaging intervals of surface shear stress are important to quantifying sediment transport because both shear stress and saltation flux are turbulent.

Atmos. Chem. Phys. Discuss., https://doi.org/10.5194/acp-2017-1090
Manuscript under review for journal Atmos. Chem. Phys.
Discussion started: 19 December 2017

Atmospheric Chemistry and Physics Discussions

In this study, we analyse the statistic behaviour of saltation using field measurements of saltation fluxes. In light of the analysis, we ask the question what the most likely values of u_{*t} and c_o are and how representative they are. We also estimate the probability distribution of the two parameters. Between 23 Feb and 14 Mar 2006, Ishizuka et al. (2008; 2014) carried out the Japan-Australian Dust Experiment (JADE) on an Australian farm. In JADE, both u_* and Q, together with a range of atmospheric and soil surface quantities, were measured with high sampling rate. The loamy sand soil surface at the JADE site was very mobile and thus the JADE data are representative to surfaces almost ideal for sand drifting. The JADE data are used in this study.

2. Method for Parameter Estimation and Data

Suppose $\tilde{X} = (\tilde{x}_1, \tilde{x}_2, ..., \tilde{x}_n)$ is a measurement vector, with $\tilde{x}_i$ being the measured value at time t_i, and A is a model with a forcing vector F and parameters β. Let the initial state of the system be i_0, then the modelled value of the system, $X = (x_1, x_2, \ldots, x_n)$, can be expressed as

$$X(\beta) = A(i_0, F; \beta) \tag{4}$$

The error vector is given by $E(\beta) = \tilde{X} - X$, here, fully attributed to β. Given $\tilde{X}$, the posterior parameter probability density function (pdf), $p(\beta|\tilde{X})$, can be estimated from the Bayes theorem:

$$p(\beta|\tilde{X}) \propto p(\beta)\, p(\tilde{X}|\beta) \tag{5}$$

where $p(\beta)$ is the prior parameter pdf, $p(\tilde{X}|\beta)$ the likelihood. If $p(\beta)$ is given, then the problem of finding $p(\beta|\tilde{X})$ reduces to finding the maximum likelihood. Assume the error residuals are independent and Gaussian distributed with constant variance, σ^2, the likelihood can be written as

$$p(\tilde{X}|\beta) = \prod_{i=1}^{n} \frac{1}{\sqrt{2\pi}\sigma} \exp\left(-\frac{(x_i - \tilde{x}_i)^2}{2\sigma^2} \right) \tag{6}$$

In this case, maximizing the likelihood is equivalent to minimizing the error, i.e.,

$$R^2(\beta) = \min \sum_i (x_i - \tilde{x}_i)^2 \tag{7}$$

This is the least-squares method for estimating β.

As an alternative, approximate Bayesian computation (ABC) method has been proposed [e.g. Vrugt and Sadegh, 2013]. It is argued that β^* should be a sample from $p(\beta|\tilde{X})$ as long as the distance between the observed and simulated data is less than a small positive value

$$\rho(\beta^*) = \left| X(\beta^*) - \tilde{X} \right| \le \varepsilon \tag{8}$$

This procedure provides an estimate of the probability distribution function for given dataset. More efficient techniques based on the same principle exist, e.g., Markov Chain Monte Carlo Simulation [Sadegh and Vrugt, 2014]. In this study, we apply the Differential Evolution Adaptive Metropolis (DREAM) algorithm proposed by Vrugt et al. (2011) for estimation of hydrologic model parameter. The algorithm integrates Differential Evolution [Storn and Price, 1997] and self-adaptive randomized subspace sampling to accelerate Markov Chain Monte Carlo simulation.

Ishizuka et al. carried out JADE between 23 Feb and 14 Mar 2006 on an Australian farm at (33º50'42.4"S, 142º44'9.0"E). A range of atmospheric variables, land surface properties, soil particle-size distributions and size-resolved sand and dust fluxes are measured. During the study period, 12 wind-erosion episodes occurred. The dataset is particular valuable in that particle size resolved sand and dust fluxes [Shao et al. 2011] were measured. The details of the experiments and datasets can be found in Ishizuka et al. [2014] and hence only a brief summary is given here.

In JADE, three Sand Particle Counters (SPCs) [Yamada et al. 2002] were used to measure saltation at the 0.05, 0.1 and 0.3 m levels with a sampling rate of 1 Hz. A SPC measures the saltation of particles in the range of 38.9 - 654.3 μm in 32 bins with mean diameters of 38.9, 54.1, 69.2 μm etc. At each measurement height, the saltation flux density ($ML^{-2}T^{-1}$), q, is obtained as the sum of q_i (saltation flux for size bin i) for the 32 size bins, i.e.

$$q = \sum_{j=1}^{32} q_j \qquad (11)$$

The saltation flux, Q, is then estimated by integrating q over height, namely,

$$Q = \int q dz \qquad (12)$$

In computing Q, we assume $q = q_0 \exp(-az)$ with q_0 and a being fitted from the measurements. As q was measured only at three heights, the vertical resolution of q is relatively poor and inaccuracies in the Q estimates are unavoidable. However, the profiles of q are well behaved and thus the inaccuracies in the Q estimates are not expected to be so large to affect the conclusions of this study.

Atmospheric variables, including wind speed, air temperature and humidity at various levels, as well as radiation and precipitation, were measured using an automatic weather station (AWS). Two anemometers were mounted at heights 0.53m and 2.16m on a mast for measuring wind speed. Also available are the Monin-Obukhov length and sensible heat fluxes. From the wind measurements, surface roughness length z_0 and friction velocity u_* are derived, assuming a logarithmic profile (with stability correction) of the mean wind. The roughness length for the experiment site is estimated to be 0.48 mm. Observations of surface soil properties, including soil temperature, soil moisture and surface cover were also made. The wind erosion model, as detailed in Shao et al. (2011), is used for computing the saltation fluxes using the JADE atmospheric and surface soil measurements as input. The essence of the saltation model component is as described in Section 1. The fraction of erodible surface area, σ_f, used in Equation (1), is estimated from photos using the technique as detailed Shao et al. (2011). For the site, the fraction of surface cover is about 0.02, almost negligible.

The resolution of Q is one second. We denote its time series as Q_{1s}. From Q_{1s}, the one-minute averages, Q_{1m}, and 30-minute averages of saltation fluxes, Q_{30m}, are derived. The resolution of

Atmos. Chem. Phys. Discuss., https://doi.org/10.5194/acp-2017-1090
Manuscript under review for journal Atmos. Chem. Phys.
Discussion started: 19 December 2017

friction velocity is one minute. We denote the one-minute averages of friction velocity as u_{*1m} and the 30-minute averages u_{*30m}.

3. Results

3.1 Statistical Features of Saltation

Fig. 1 shows the time series of Q_{1m} and u_{*1m}, and Fig. 2 Q_{30m} and u_{*30m}. The figures show that both Q and u_* significantly fluctuate, but the amplitude of Q_{1m} fluctuations is several times of that of Q_{30m} fluctuations.

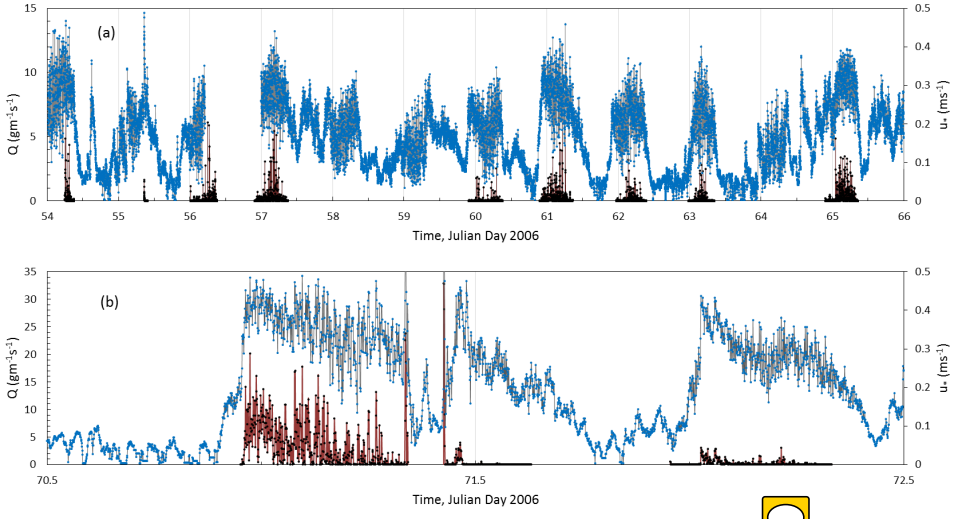

Figure 1: Observed time series of 1-min averaged saltation flux, Q ($gm^{-1}s^{-1}$), and friction velocity, u_* (ms^{-1}). Note that the axes in (b) have different scales as in (a).

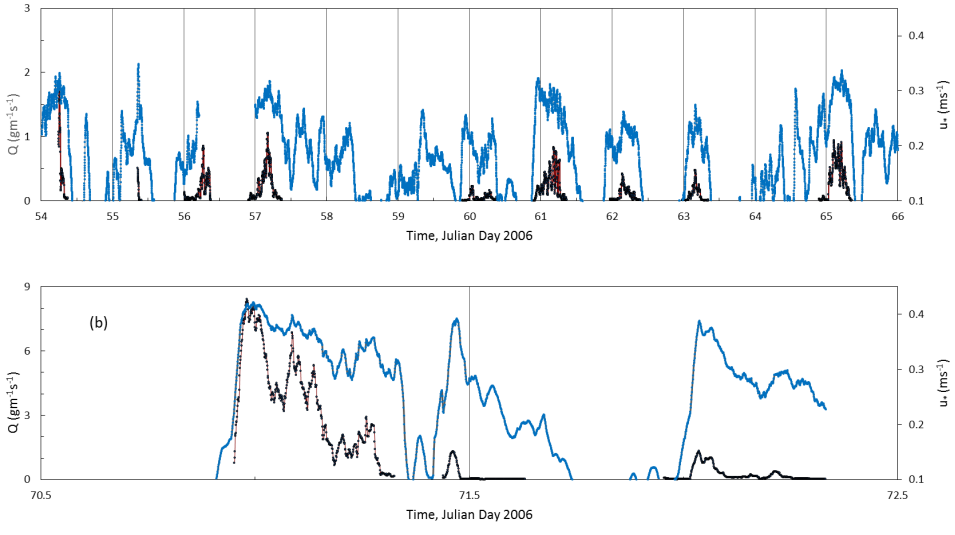

Atmos. Chem. Phys. Discuss., https://doi.org/10.5194/acp-2017-1090
Manuscript under review for journal Atmos. Chem. Phys.
Discussion started: 19 December 2017

Atmospheric Chemistry and Physics Discussions

Figure 2: As Fig. 1, but for running means over 30-min intervals.

In Fig. 3, Q is plotted against u_*^3. Several interesting features can be identified. For the majority of the points, the $Q \sim u_*^3$ relationship appears to hold, but this relationship can vary significantly even for the same data set from event to event. For example, large differences exist between day 62 (a day of intensive wind erosion) and day 72 (a day of weak wind erosion), as seen in both Fig. 3a and Fig. 3b. Also hysteresis can be observed in the saltation flux and friction velocity relationship (Fig. 3c): during an erosion event, for the same friction velocity, saltation is much stronger in the strengthening than in the weakening phase. There may be many reasons for the hysteresis in the relationship between sediment flux and friction velocity but the most likely are the differences in atmospheric turbulence (e.g. more gusty in the strengthening than in the weakening phase) and time-varying surface conditions (e.g. particle sorting and aerodynamic roughness).

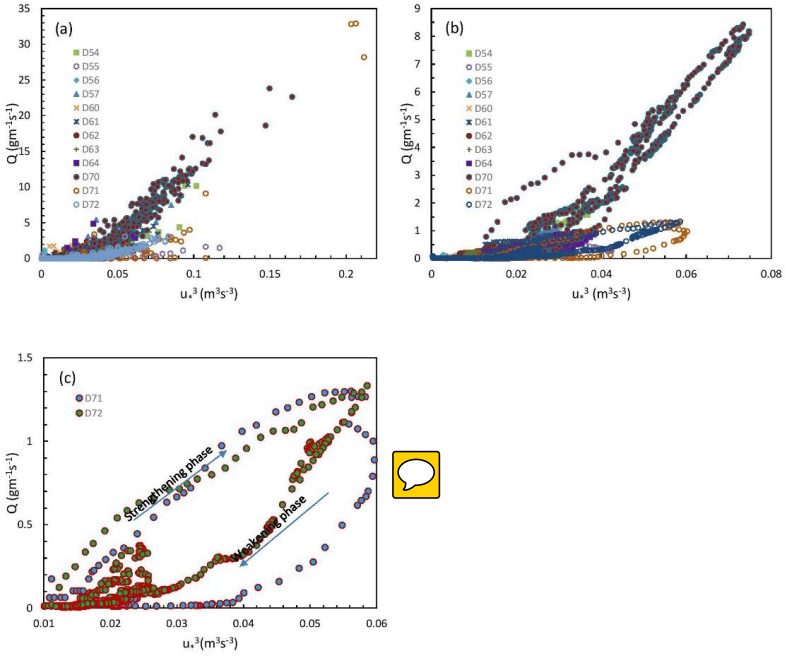

Figure 3: (a) Saltation flux, Q ($gm^{-1}s^{-1}$), plotted against friction velocity, u_*^3 (m^3s^{-3}), for 1-minute averages; (b) As (a), but for 30-minute averages; (c) As (b), but enlarged to illustrated saltation hysteresis.

How well the saltation model performs, whether u_{*t} and c_o are universal and how they are probabilistically distributed must depend on the turbulent properties of saltation. As the JADE saltation fluxes are sampled at 1 Hz, we can use the data to reveal (to some degree) the statistical behavior of saltation. In Fig. 4, the pdfs of the saltation fluxes for different particle size groups are plotted, computed using Q_{1s} and Q_{1m}. It is seen that the pdfs generally behaves like

$$p(Q) \propto Q^{-\alpha} \qquad (13)$$

Atmos. Chem. Phys. Discuss., https://doi.org/10.5194/acp-2017-1090
Manuscript under review for journal Atmos. Chem. Phys.
Discussion started: 19 December 2017

Atmospheric Chemistry and Physics Discussions

In case of Q_{1s}, there seems to be a distinct change in α at a critical value of $Q_c \sim 3$ gm^{-1}s^{-1}, with $\alpha = 0.8 \sim 0.9$ for $Q < Q_c$ and $\alpha = 4.0$ for $Q > Q_c$. The pdfs derived from Q_{1m} appear to be somewhat different, although the basic functional form is as given by Equation (13). In this case, α is about 1 and drops off to about 2 for large Q values. Fig. 4 shows that the pdfs of Q depends quite significantly on the interval of time averaging. Fig. 4 also shows that after averaging, smaller saltation fluxes become more likely. This is because the time series of Q_{1s} is more intermittent (see also Fig. 6).

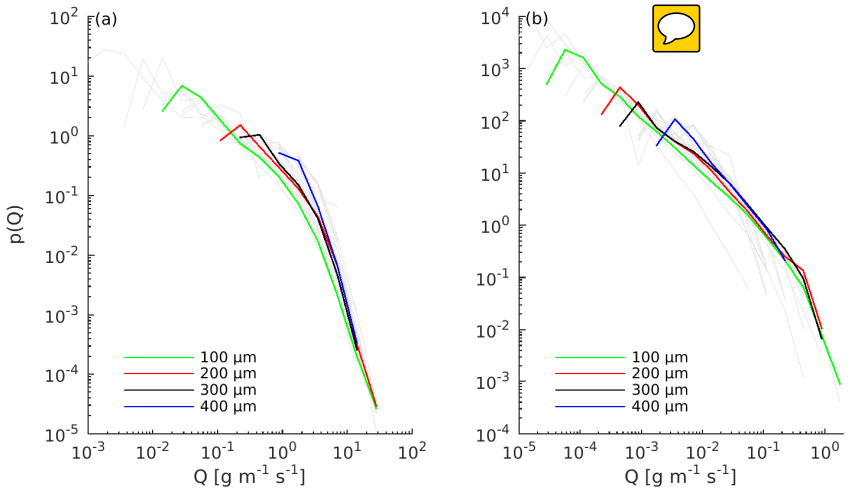

Figure 4: (a) Probability density functions of saltation flux averaged over 1 second; (b) as (a), but for saltation fluxes averaged over 1 minute.

In theory, $p(Q)$ can be derived from the pdf of u_*, $p(u_*)$. From Equation (2), we have

$$\frac{dQ}{du_*} = c_0 \frac{\rho}{g}\left(3u_*^2 + 2u_* u_{*_t} - u_{*_t}^2\right) \quad \text{for} \quad u_* > u_{*_t} \tag{14}$$

~~It follows that~~

$$p(Q) = \begin{cases} p(u_*)\dfrac{du_*}{dQ} & \text{for} \quad u_* > u_{*_t} \\ 0 & \text{for} \quad u_* \le u_{*_t} \end{cases} \tag{15}$$

Fig. 5a shows the $p(u_*)$ estimated from u_{*1m} and Fig. 5b $p(Q)$ estimated from Q_{1m}. It is seen that $p(u_*)$ can be well fitted with a Weibull distribution. We computed $p(Q)$ using Equation (15) with the fitted $p(u_*)$, assuming $u_{*_t} = 0.2$ ms^{-1} and $c_o = 2.6$. It is seen that while the observed and modelled $p(Q)$ only have qualitative similarities but are profoundly different. Fig. 5 shows that even if the saltation model cannot reproduce the $p(Q)$ if u_{*_t}. For example, the model fails to predict the frequent weak saltation occurring when u_* is below the specified threshold.

Atmos. Chem. Phys. Discuss., https://doi.org/10.5194/acp-2017-1090
Manuscript under review for journal Atmos. Chem. Phys.
Discussion started: 19 December 2017

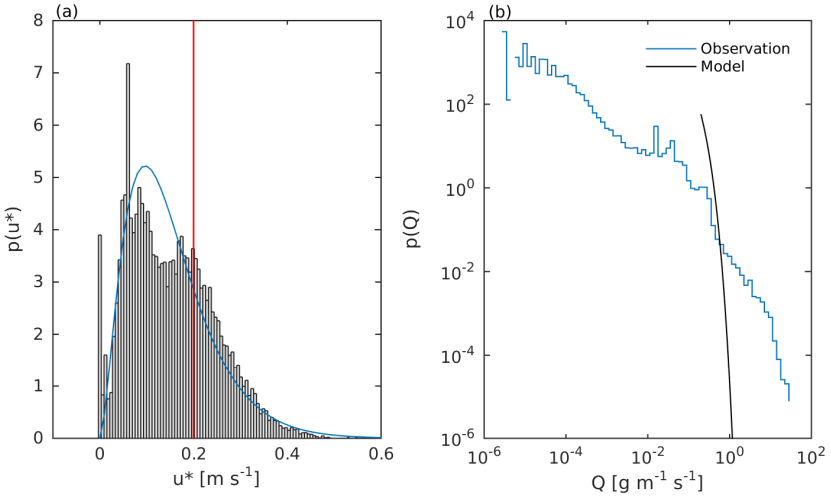

Figure 5: (a) Probability density functions of friction velocity, $p(u_*)$, plotted against u_* (bars). To compute $p(u_*)$, u_{*1m} is used; a Weibull distribution (blue line) is fitted to $p(u_*)$; the red line marks the assumed threshold friction velocity. (b) Probability density function of Q, $p(Q)$, estimated using Q_{1m} (blue) and using Equation (15) (black).

Also, the soil particle size distribution can influence $p(Q)$. In JADE, soil samples from the experiment site were collected and the psds were analyzed in laboratory. Depending on the methods used, the soil texture can be classified as sandy loam (clay 0.33%, silt 25% and sand 74.67%) or loamy sand (clay 11%, silt 35% and sand 54%). The soil at the observation site is bimodal with one psd maximum at about 180 μm and another at about 500 μm (not shown). The relatively large $p(Q)$ at about $Q_{1m} = 10^{-1}$ $gm^{-1}s^{-1}$ is related to the psd maximum at $d = 180$ μm.

Following Stout and Zobeck [1997], the intermittency of saltation, γ_{int}, is defined as the fraction of time during which saltation occurs at a given point in a given time period. The latter authors assumed that saltation is expected to occur only in the time windows when friction velocity exceeds the threshold friction velocity. Therefore, suppose $p(u_*)$ is known, then γ_{int} is

$$\gamma_{\text{int}} = 1 - \int_0^{u_{*t}} p(u_*)du_*$$

This definition of γ_{int} is problematic, because u_{*t} here is fixed. Stout and Zobeck [1997] used the counts per second of sand impacts on a piezoelectric crystal saltation sensor as a measure of saltation activity and found that γ_{int} rarely exceeds 0.5.

We examined γ_{int} using the JADE data. First, γ_{int} is computed using Q_{1m} conditionally sampled for $u_* > u_{*c}$, with u_{*c} successively varied from small to large. In Fig. 6a, γ_{int} is plotted as a function of u_{*c}. It is seen that on one-minute intervals, γ_{int} has a maximum of about 0.25 for small u_{*c} and decreases to zero at about $u_{*c} = 0.3$ ms^{-1}. This shows that saltation intermittency mainly occurs under weak wind conditions. If γ_{int} is computed using Q_{1s}, then its maximum reaches about 0.4, similar to that reported in Stout and Zobeck [1997]. For the one-second case, we cannot plot γ_{int} as a function of u_{*c}, because u_* is not available at such high frequency. Fig. 6b shows (the maximum of) γ_{int} as function of particle size for the one-second, one-minute and

Atmos. Chem. Phys. Discuss., https://doi.org/10.5194/acp-2017-1090
Manuscript under review for journal Atmos. Chem. Phys.
Discussion started: 19 December 2017

Atmospheric Chemistry and Physics Discussions

30-minute cases. In general, γ_{int} increases with particle size, i.e., the saltation of larger particles is more intermittent. Also, γ_{int} decreases with increased averaging time intervals, implying that the small scales features of turbulence play an important role in intermittent saltation.

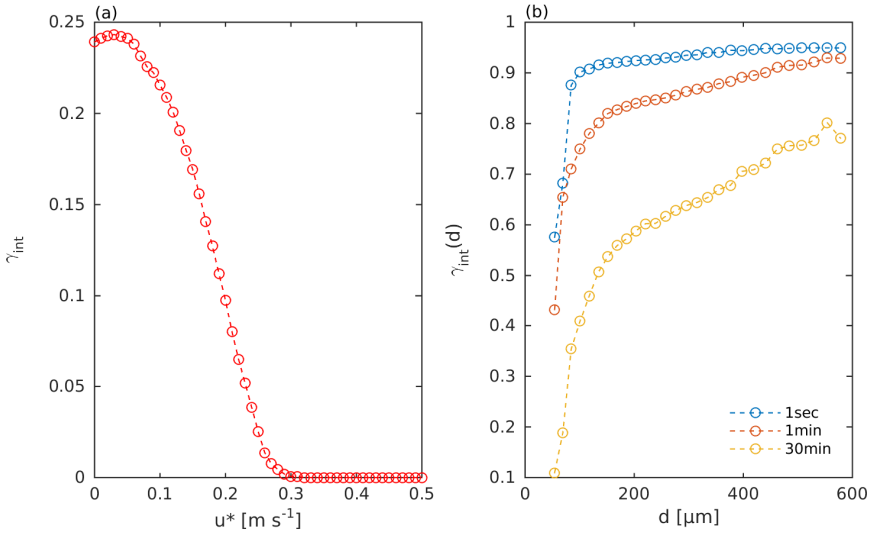

Figure 6: (a) Saltation intermittency, γ_{int}, computed using Q_{1m} conditionally sampled for $u_* > u_{*c}$; (b) γ_{int} as a function of particle size for the one-second, one-minute and 30-minute cases.

Fig. 7 shows the power spectra of Q and u_* (Fig. 7a) as well their co-spectrum (Fig. 7b). The power spectrum of Q is computed using both Q_{1s} and Q_{1m}, that of u_* with u_{*1m}. It is seen that the power spectra of Q and u_* have qualitatively very similar behaviour. Both have a maximum at about 10^{-5} Hz, a minimum at about 10^{-4} Hz and another maximum at about 2×10^{-3} Hz. The maximum at 10^{-5} Hz is related to the diurnal to synoptic events which drive the wind erosion episodes, the minimum at 10^{-4} Hz is due to the lack of turbulent winds at the time scale of several hours, while the maximum at 2×10^{-3} Hz is caused by the minute-scale gusty winds/large eddies in turbulent flows. Also the Q-u_* co-spectrum shows that Q and u_* are most strongly correlated on diurnal/synoptic and gust/large-eddy time scales. The saltation spectrum computed using Q_{1s} reveals again the maximum at 2×10^{-3} Hz. However, the power of Q spectrum rapidly decreases with frequency and become relatively weak on time scales smaller than ~ 10 s.

Atmos. Chem. Phys. Discuss., https://doi.org/10.5194/acp-2017-1090
Manuscript under review for journal Atmos. Chem. Phys.
Discussion started: 19 December 2017

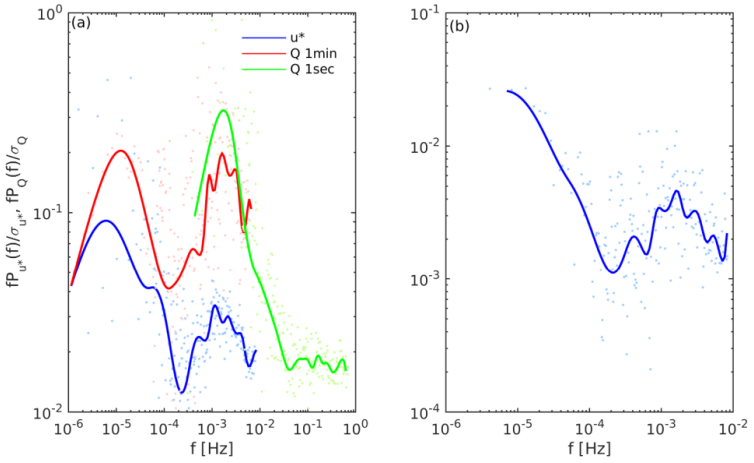

Figure 7: (a) Normalized power spectrum of friction velocity (blue) computed with u_{*1m}, together with the normalized power spectrum of saltation flux computed with Q_{1m} (red) and Q_{1s} (green). (b) Normalized Q-u_* co-spectrum, computed using with Q_{1m} and u_{*1m}. In both (a) and (b), dots are unsmoothed spectra, while curves are smoothed spectra.

4.2 Estimates of Saltation Model Parameters

Given the turbulent nature of saltation, it is rational to treat u_{*t} and c_0 in the saltation model to be parameters obeying certain probability distributions. To examine the behavior of these parameters, we introduce two coefficients r_{c0} and $r_{u*t,}$ and multiply them respectively to c_0 and u_{*t} in Equation (2). They are then varied to generate a model estimate of Q using Equations (2) and (3) with observed u_* and the theoretical values of u_{*t} and c_0. We denote the time series of the modelled saltation flux as $Q_{M,i,}$ (i=1,N) and of the corresponding measurement $Q_{D,i}$. The absolute error, δQ_A, and Nash coefficient, I_{Nash}, are used as measures for the goodness of the agreement between the model and the measurement. They are defined as,

$$\delta Q_A = \frac{1}{N}\sum |a_i|$$

$$I_{Nash} = (1 - \sum a_i^2 / \sum b_i^2)$$

with

$$a_i = Q_{M,i} - Q_{D,i}$$

$$b_i = Q_{M,i} - \frac{1}{N}\sum Q_{M,i}$$

$$c_i = \begin{cases} a_i / Q_{M,i} & Q_{M,i} \neq 0 \\ 0 & \text{else} \end{cases}$$

The prior pdfs of r_{c0} and r_{u*t} are assumed to be uniform. In the numerical experiment, we randomly generate r_{c0} and r_{u*t} and seek their values, such that $\delta Q_A \leq \varepsilon$ and $I_{Nash} > \eta$. These

Atmos. Chem. Phys. Discuss., https://doi.org/10.5194/acp-2017-1090
Manuscript under review for journal Atmos. Chem. Phys.
Discussion started: 19 December 2017

Atmospheric Chemistry and Physics Discussions

experiments are repeated for Q_{1m} and Q_{30m}. The plots of δQ_A and I_{Nash} as functions of r_{c0} and r_{u*t} show that for certain values of r_{c0} and r_{u*t}, the above conditions are satisfied. Fig. 8 shows that for Q_{1m}, the best simulation is achieved with r_{c0} = 1.23 and r_{u*t} = 1.05, while for the Q_{30m}, with r_{c0} = 0.94 and r_{u*t} = 0.91. This shows that while the "optimal" estimates of u_{*t} and c_0 are close to the corresponding theoretic values, they are dependent on the time averaging intervals, with both u_{*t} and c_0 being larger for shorter averaging intervals.

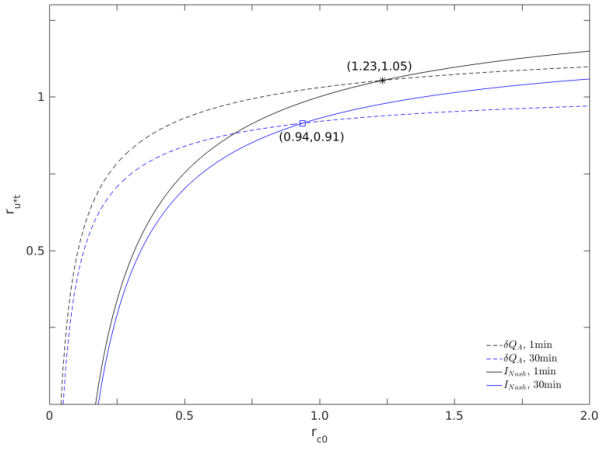

Figure 8: δQ_A and I_{Nash} are both functions of r_{c0} and r_{u*t}. Along the dashed curves, the condition $\delta Q_A = \min$ is satisfied and along the solid curves the condition $I_{Nash} = \max$ is satisfied. The curves are estimated with both one-minute and 30-minute averaged saltation fluxes.

The parameter pdfs $p(r_{u*t})$ and $p(r_{c0})$ estimated using the DREAM algorithm are shown Fig. 9. All pdfs are fitted to a Γ-distribution. As seen in Fig. 9a and 9c, the most frequent r_{u*t} values are respectively 1.12 and 1.04 for Q_{1m} and Q_{30m}, close to the estimates of 1.05 and 0.91 found in Fig. 8. For Q_{1m}, r_{u*t} scatters in the range of ~1.12 ± 0.2 and for Q_{30m} in the range of ~1.04 ± 0.3. This implies that sometimes saltation occurs when u_* is below the theoretic u_{*t} value and sometimes saltation does not occur even when u_* is above the theoretic u_{*t}, as already seen in Fig. 6a. In the case of $p(r_{c0})$ (Fig. 9c and 9d), the most frequent values of r_{c0} for Q_{1m} and Q_{30m} are respectively 1.04 and 0.92, close to the optimal estimates of 1.23 and 0.94 found in Fig. 8. But r_{c0} scatters over a wide range, for instance, for Q_{30m} between 0.5 and 5, i.e., c_0 is a rather stochastic parameter.

Atmos. Chem. Phys. Discuss., https://doi.org/10.5194/acp-2017-1090
Manuscript under review for journal Atmos. Chem. Phys.
Discussion started: 19 December 2017

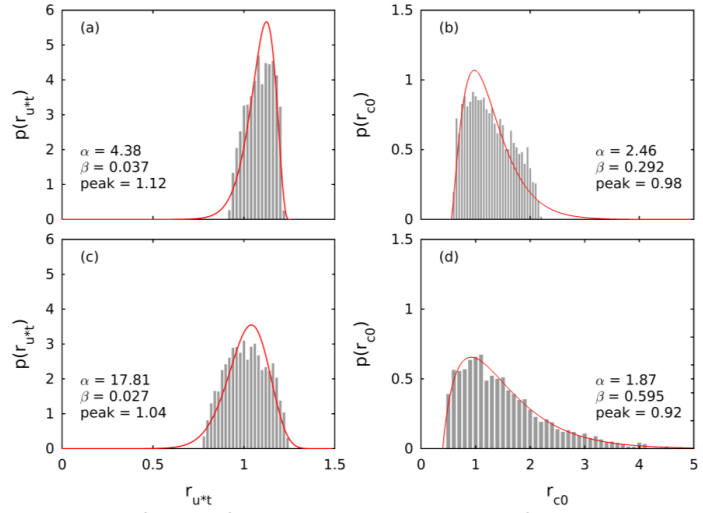

Figure 9: (a) Parameter pdf $p(r_{u*t})$ for 1-min averaged saltation fluxes; (b) as (a), but for $p(r_{c0})$; (c) and (d), as (a) and (b), but for 30-min averaged saltation fluxes.

In nature, many factors influence sediment transport, but the stochasticity of the parameters is determined primarily by the turbulent fluctuations of friction velocity (representing surface shear stress), the randomness of threshold friction velocity, and soil particle size distribution (representing particle response to forcing). Studies have shown, for instance, that small changes in soil moisture can have large influences on saltation [Ishizuka et al. 2008] and soil moisture in the very top soil layer can vary significantly over relatively short time periods. Over the period of 18 days this study is based on soil moisture varied. In this study, the influence of soil moisture on saltation is accounted for via Equation (1) using the soil moisture measurements in the top 0.05m layer (see also Fig. 4a in Shao et al. 2011). The uncertainty in the wind erosion parameters arising from soil moisture is most likely reflected in the stochasticity of u_{*t}.

The stochasticity of c_0 is more likely related to turbulence and particle size. To show this, we divided the time series of the saltation fluxes into two subsets, one with $Q_{D,i} \leq 3$ gm^{-1}s^{-1} representing weak saltation and one with $Q_{D,i} > 3$ gm^{-1}s^{-1} representing significant saltation. This separation is arbitrary but sufficient for making the point that wind erosion parameters depend on u_* which is a measure of turbulence intensity. The parameter pdfs, $p(r_{u*t})$ and $p(r_{c0})$, for the subset $Q_{D,i} \leq 3$ gm^{-1}s^{-1} is shown in Fig. 10. For Q_{1m} and Q_{30m}, the most frequent r_{u*t} values are now respectively 0.99 and 0.85, somewhat smaller than the estimated values for the full set (see Fig. 9). In comparison, the most frequent r_{c0} values are now respectively 0.30 and 0.29, much smaller than for the case when the full set is considered (see Fig. 9). This suggests that c_0 has a dependency on u_* and is smaller for smaller u_* when saltation is more intermittent, as also seen in Fig. 6a.

Atmos. Chem. Phys. Discuss., https://doi.org/10.5194/acp-2017-1090
Manuscript under review for journal Atmos. Chem. Phys.
Discussion started: 19 December 2017

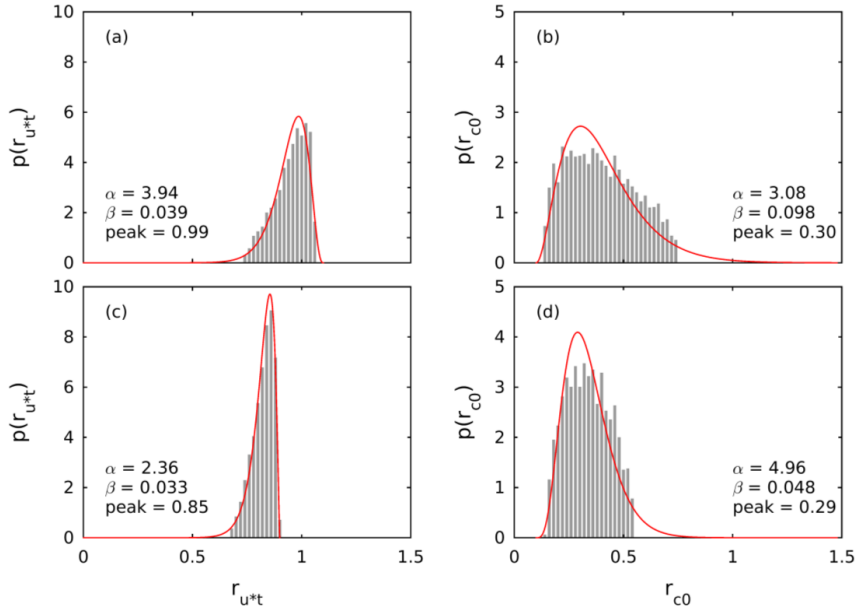

Figure 10: As Fig. 9, but estimated using the time series of saltation fluxes which satisfy $Q_{D,i} \leq 3$ gm^{-1}s^{-1}.

We fitted the pdfs, $p(r_{u*t})$ and $p(r_{c0})$, for individual particle size bins. It is found that the most frequent r_{u*t} values do not differ substantially among the particle sizes, but r_{c0} depends systematically on particle size. For example, the most frequent r_{c0} values for 100.7, 151.2, 203.3, 314.5 and 397.7 μm are respectively 0.48, 1.31, 1.65, 3.06 and 4.00. These values are obtained by first estimating $p(r_{c0})$ for the individual particle size bins with the measured saltation flux for the corresponding bins and then normalizing $p(r_{c0})$ with the mass fraction of the size bins of the parent soil. A least squares curve fitting shows that the most frequent r_{c0} value depends almost linearly on particle size:

$$r_{c_0} = 0.012d - 0.62 \qquad (16)$$

for the particle size range (100 to 400 μm) we tested, with d being particle size in μm.

We have shown that both u_{*t} and c_0 satisfy certain pdfs which depend on the properties of the surface, atmospheric turbulence and soil particle size. Fig. 9 shows that for a fixed choice of u_{*t} and c_0, even if they are "optimally" chosen, a portion of the measurements cannot be represented by the model. Then, how does the saltation model perform if a single fixed u_{*t} and a single fixed c_0 are used as is often the case in aeolian models? The $p(Q)$ computed using the model and derived from the JADE measurements are shown for Q_{1m} and Q_{30m} in Fig. 11. In this case, the saltation model is applied to the individual particle size groups and the total (particle-size integrated) saltation flux is computed using the u_{*t} and c_0 optimally estimated. Fig. 11 shows that the model over predicts and probability of large Q, but under predicts the probability of small Q in both cases of Q_{1m} and Q_{30m}.

Atmos. Chem. Phys. Discuss., https://doi.org/10.5194/acp-2017-1090
Manuscript under review for journal Atmos. Chem. Phys.
Discussion started: 19 December 2017

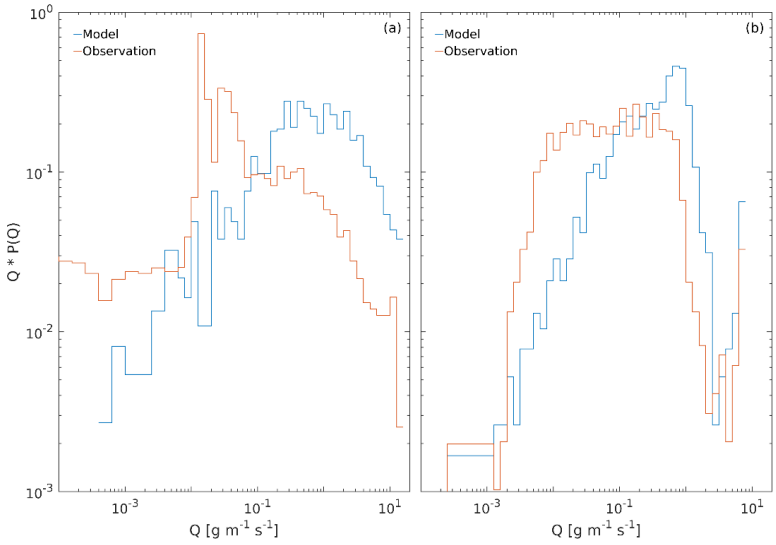

Figure 11: (a) Probability density functions of observed Q and simulated Q for 1-min averages; (b) as (a), but for 30-min averages.

5. Summary

In this paper, we have used the JADE data of saltation fluxes (resolution one second) and frictional velocity (resolution one minute) to analyze the statistical behavior of turbulent saltation and estimate the probability distribution of two of the most important parameters, namely, the threshold friction velocity, u_{*t}, and saltation coefficient, c_0, in a saltation model.

Saltation fluxes show a rich variations on different scales. It is found that while the widely used $Q \sim u_*^3$ relationship holds in general, it can vary significantly between different wind erosion events. In several wind erosion events observed in JADE, saltation hysteresis occurred. We examined the probability density function of the saltation fluxes, $p(Q)$, and found that it generally behaves like $Q^{-\alpha}$. For Q_{1s}, there is a distinct change in α at $Q = 3 \sim 4$ gm^{-1}s^{-1} with $\alpha = 0.8 \sim 0.9$ for smaller Q and $\alpha = 4.0$ larger Q. It is shown that $p(Q)$ is dependent on the averaging time intervals as a consequence of saltation intermittency.

We defined saltation intermittency, γ_{int}, as the fraction of time during which saltation occurs at a given point in a given time period, and computed γ_{int} using the JADE saltation flux measurements. For Q_{1m} conditionally sampled with $u_* > u_{*c}$, it is found that γ_{int} has a maximum of about 0.25 for small u_{*c} and decreases to zero at about $u_{*c} = 0.3$ ms^{-1}. This shows that saltation intermittency mainly occurs under weak wind conditions. The γ_{int} computed using Q_{1s} has a maximum of about 0.4. We have also computed γ_{int} as a function of different particle sizes and found that γ_{int} in general increases with particle size.

The power spectra of saltation flux and friction velocity are found to have qualitatively similar behaviour. Both have a maximum at about 10^{-5} Hz, a minimum at about 10^{-4} Hz and another maximum at about $2\text{x}10^{-3}$ Hz. The maximum at 10^{-5} Hz is related to the diurnal to synoptic events which drive wind erosion episodes, the minimum at 10^{-4} Hz is due to the lack of turbulent wind fluctuations at the time scale of several hours, while the maximum at $2\text{x}10^{-3}$ Hz is caused

by the minute-scale gusty winds/large eddies in turbulent flows. The power of the saltation rapidly decreases with frequency and become relatively weak at frequencies of 0.1 Hz.

The posterior pdfs of the two parameters are estimated using the DREAM algorithm applied to the JADE saltation flux measurements. While both u_{*t} and c_0 have clear physical interpretations, they appear to be dependent on the intervals of time averaging. Both u_{*t} and c_0 for the 1-min averages are larger than for the 30-min averages. The pdf of u_{*t} shows that it has a most frequent value close to the theoretic value, but can vary in a range of 20 to 30%. Therefore, the use of the most frequent value of u_{*t} in the saltation model seems to be reasonable. In contrast, the pdf of c_0 shows that it scatters over a much wider range. This suggests that it is rather unlikely that a universal c_0 exists and the use of the most frequent value of c_0 would not reduce the scatter between the model and the data. The likely reason for the relatively large uncertainty in c_0 may be that it is parameter depending on additional factors (e.g. friction velocity and soil particle size distribution). It may also be that saltation in reality is never in equilibrium as Bagnold (1941), Kawamura (1964) and Owen (1964) conceptualized, because due to turbulent fluctuations, sand grains are continuously entrained at different rates into the airflow and a continuous flow and particle-motion feedback takes place. As a consequence, it is difficult to treat c_0 as a universal constant.

Acknowledgement: This research is funded by the National Natural Science Foundation of China (Control mechanism of groundwater-soil-vegetation continuum on dust emission in desert playas, No. 41571090). The data used in this study are obtained in JADE (the Japan Australian Dust Experiment) by M. Ishizuka, M. Mikami, J. F. Leys, Y. Yamada, and S. Heidenreich. We are grateful to P. Schlüter and Q. Xia for support with data processing.

References:

Bagnold, R.A. (1941): The Physics of Blown Sand and Desert Dunes. Methuen, London, 265pp.

Butterfield, G. R. (1991): Grain transport rates in steady and unsteady turbulent airflows. Acta Mechanica, Suppl. 1, 97-122.

Davidson-Arnott, R. G. D., and B. O. Bauer (2009): Aeolian sediment transport on a beach: Thresholds, intermittency, and high frequency variability. Geomorphology 105: 117–126.

Dupont, S., G. Bergametti, B. Marticorena, and S. Simoëns (2013), Modeling saltation intermittency, J. Geophys. Res. Atmos., 118, 7109–7128, doi:10.1002/jgrd.50528.

Ellis, J. T., D. Sherman, E. J. Farrell and B. L. Li (2012): Temporal and spatial variability of aeolian sand transport: Implications for field measurements. Aeolian Research 3(4):379-387. DOI: 10.1016/j.aeolia.2011.06.001,

Fecan, F., Marticorena B., Bergametti G. (1999) Parametrization of the increase of the aeolian erosion threshold wind friction velocity due to soil moisture for arid and semi-arid areas. Annales Geophysicae 17:149–157

Ishizuka, M., Mikami, M., Leys, J. F., Yamada, Y., Heidenreich, S., Shao, Y., McTainsh, G. H. (2008): Effects of soil moisture and dried raindroplet crust on saltation and dust emission. J. Geophys. Res. 113, D24212, doi:10.1029/2008JD009955

Ishizuka, M., Mikami, M., Leys, J. F., Shao, Y., Yamada, Y. and Heidenreich, S. (2014): Power law relation between size-resolved vertical dust flux and friction velocity measured in a fallow wheat field. Aeolian Research 12:87-99. DOI: 10.1016/j.aeolia.2013.11.002

Klose, M., Y. Shao, X. Li, H. Zhang, M. Ishizuka, M. Mikami, and J. F. Leys (2014): Further development of a parameterization for convective turbulent dust emission and evaluation based on field observations. J. Geophys. Res. Atmos. 119, 10,441–10,457, doi:10.1002/2014JD021688.

Kok, J.F., N.M. Mahowald, G. Fratini, J.A. Gillies, M. Ishizuka, J.F. Leys, M. Mikami, M.S. Park, S.U. Park, R.S. Van Pelt, T.M. Zobeck (2014): An improved dust emission model – Part 1: model description and comparison against measurements. Atmos. Chem. Phys. 14, 13023–13041

Kawamura, R. (1964): Study of sand movement by wind. In: Hydraulic Eng. Lab. Tech. Rep., University of California, Berkeley, HEL-2-8, pp 99–108

Namikas, S. L., B. O. Bauer and D. Sherman (2003): Influence of averaging on shear velocity estimates for aeolian transport modeling. Geomorphology 53, 235-246, DOI: 10.1016/S0169-555X(02)00314-8

McKenna-Neuman, C., N. Lancaster, and W. G. Nickling. 2000. The effect of unsteady winds on sediment transport on the stoss slope of a transverse dune, Silver Peak, NV, USA. Sedimentology 47: 211–226.

Owen, R. P. (1964): Saltation of uniform grains in air. J. Fluid. Mech. 20, 225–242.

Raupach, M.R., Gillette D.A. and Leys J.F. (1993): The effect of roughness elements on wind erosion thresholds. J. Geophys. Res. 98:3023–3029.

Sadegh, M. and J. A. Vrugt (2014): Approximate Bayesian computation using Markov Chain Monte Carlo simulation: DEARM$_{(ABC)}$. Water Resour. Res. 50, doi:10.1002/2014WR015386

Shao, Y. and Lu H. (2000): A simple expression for wind erosion threshold friction velocity. J. Geophys. Res. 105:22,437–22,443

Shao, Y., M. Ishizuka, M. Mikami, and J. F. Leys (2011): Parameterization of size-resolved dust emission and validation with measurements. J. Geophys. Res., 116, D08203, doi:10.1029/2010JD014527

Shao, Y. and Mikami, M. (2005): Heterogeneous Saltation: Theory, Observation and Comparison. Boundary-Layer Meteorol. 115:359. doi:10.1007/s10546-004-7089-2

Sherman, D., B. L. Li, J. T. Ellis and C. Swann (2017): Intermittent aeolian saltation: A protocol for quantification. Geographical Review 1–19. DOI: 10.1111/gere.12249.

Storn, R. and Price, K. (1997): Differential Evolution – a simple and efficient heuristic for global optimization over continuous spaces. J. Global Optim. 11, 341-359

548 Stout, J. E. and T. M. Zobeck (1997): Intermittent saltation. Sedimentology 44, 959-970
549
550 Vrugt, J. A., ter Braak, C. J. F., Diks, G. H., Robinson, B. A., and Hyman, J. M. (2011):
551 Accelerating Markov Chain Monte Carlo Simulation by Differential Evolution with Self-
552 Adaptive Randomized Subspace Sampling. Int. J. Nonlin. Sci. Num. 10(3), 273-290.
553 doi:10.1515/IJNSNS.2009.10.3.273
554
555 Vrugt, J. A. and M. Sadegh (2013): Toward diagnostic model calibration and evaluation:
556 Approximate Bayesian computation. Water Resour. Res. 49, 4335-4345.
557 doi:10.1002/wrcr.20354
558
559 White, B.R. (1979): Soil transport by winds on Mars. J. Geophys. Res. 84, 4643-4651
560
561 Yamada Y., Mikami M., Nagashima H. (2002): Dust particle measuring system for streamwise
562 dust flux. J. Arid Land Studies 11(4): 229–234